VILNIUS TECH
Vilnius Gediminas Technical University

AVIATION
ISSN: 1648-7788 / eISSN: 1822-4180
2023 Volume 27 Issue 1: 57–66
https://doi.org/10.3846/aviation.2023.18629

VIBROACOUSTIC SOUNDPROOFING FOR HELICOPTER INTERIOR

Pavithra NAGARAJ [1*], Adham Ahmed Awad Elsayed ELMENSHAWY [1], Iyad ALOMAR [2]

[1]*Riga Technical University, Ķipsalas iela 6A, LV-1048 Rīga, Latvia*
[2]*Transport and Telecommunication Institute, Lomonosova 1, LV-1019 Riga, Latvia*

Received 15 May 2022; accepted 12 October 2022

Abstract. As VIP passengers generally want to fly civil and executive jets where vibratory and acoustic environment is smoother than on the normal jets. Helicopter interior noise is generated by main and tail rotors, engines, main gearbox, and aerodynamic turbulence (Lu et al., 2018). Because of these sources, the tonal and broadband noise is incredibly high and needs to be reduced. Conventional passive system (soundproofing) is the best way to control the acoustic of the cabin whereas active systems (active vibration and noise control) are not completely reliable or applicable. The design of the soundproofing may be researched by simulation using one of these programs: ANSYS, SOLIDWORKS 2020 and ACOUSTIC analysis Vibroacoustic Monitoring (VAM) approach. The analyses were performed from frequency ranges, 5-10Hz and 0-2000Hz then transformed into frequency velocity domain using Proudman's equations (Lu et al., 2017). Soundproofed ANSYS models are validated using instantaneous sound pressure levels measured within the helicopter during flight. The acoustic detection method for GAZELLE is also performed successfully in SOLIDWORKS for aluminum alloy and titanium alloy, this proves the relationship between acoustic power levels and material configuration. The noise coefficient responses of interior materials are used as main index for soundproofing helicopter interiors. The results of this research can be used for implementation of VAM approach for soundproofing helicopter interiors.

Keywords: vibro-acoustic, soundproofing, sound pressure level, VAM approach, DAVA approach, sound absorption coefficient material.

Introduction

Interior soundproofing is a wide topic, as there are several methods to achieve the soundproofing. Some of these methods are but not limited to introducing extra insulation materials, optimizing the structure, optimizing the materials used, introducing struts in gearbox, and the long list goes on. Moreover, there are a lot of ways that have already been experimented. Most of these methods have succeeded to proof the theory worth to be applied on a practical level (Wikipedia, n.d.). Some methods are more effective in soundproofing yet, they are expensive to produce. Regardless, using such techniques in VIP helicopters renders them as cost-effective (This Day in Aviation, 2021). Over the last 10 years, the focus of Adaptive Mesh Refinement (AMR) for NASA's vertical lift research was to adddynamic mesh adaption capability to the structured Navier–Stokes flow solver "OVERFLOW2", initially for off-body mesh and then subsequently for near-body mesh (Yamauchi, 2018). The mesh adaption approach was to develop a solution-adaptive capability using the existing chimera zonal grid framework in OVERFLOW2. While this is less rigorous than an adjoint-based approach as used in the unstructured Navier–Stokes flow solver, "FUN3D" (Park, 2011). The solution-based approach is much simpler to implement with a lower computational cost and is more conducive to dynamic mesh adaption for unsteady flow needed for rotor wakes (Simon & Savage, 1975). This research by Holst and Pulliam (2009) demonstrated that this dynamic local mesh refinement approach used approximately five times less computational resources than a uniformly refined mesh. The mesh adaption work was followed by an improved off-body solution adaption capability implemented in OVERFLOW2 by (Buning & Pulliam, 2011). This new capability was based on the original work done by Meakin (1995) and provided for the automatic creation of multiple levels of finer Cartesian off-body meshes. The adaption capability was also coupled with load-balancing and an in-memory solution

*Corresponding author. E-mail: *pavithra.nagaraj@rtu.lv*

interpolation procedure, providing good performance for time-accurate simulations on parallel computer platforms (Agusta Westland European Aviation, 2013). The soundproofing is acquired through performing changesin design and materials either in the cabin interiors or exteriors. Vibroacoustic soundproofing of helicopter interiors wereperformed focusing mainly on the Aerospatiale Gazelle which is a light helicopter that people use for civil chartered flight purposes (Mucchi et al., 2012). As the study was conducted on a Fenestron based first helicopter Gazelle, similar study was conducted on Airbus H135 where they used the Fenestron structure (Vario Helicopter, 2020). For finding out the impact on the conventional tail rotor helicopters, the simulation was also performed on a Bell 429 rotor craft. Focusing on the aim for soundproofing, finding and conclusions were made according to the chosen materials (Globalair, 2020). While it is useful to be able to model / predict thenoise environment of the rotorcraft within the fuselage, it is at least crucial to identify ways of mitigating that noise as effectively as possible (Pierro et al., 2009). It significantly reduces the likelihood adverse effects on vehicle performance due to as increasedcost and/or complexity, increased weight penalties etc. (Helicopter University, 2018). The calculation and simulations will be taking place in two software namely, SOLIDWORKS 2020 and ANSYS 19.2. The process on the ANSYS takes place through a series of processes, starting from setting the units, carried on by model importing, setting the geometry, setting load and boundarycondition, creating computational domain, introducing finite element meshing, calculation of inputs, coordinate systems,connection status, named selection and special harmonic acoustic analysis (Lu et al., 2018). This approach has been successfully used forthe GAZELLE trim design evaluating acoustic performances versus weight and costs (Airvectors, 2021). Soundproofed ANSYS models arethen definitely validated using instantaneous sound pressure levels measured within the helicopter during flight. The acoustic detection method for GAZELLE was also performed successfully in SOLIDWORKS for aluminum alloy and titanium alloy. And this proves the relationship between acoustic powers and material configuration. The noise coefficient responses of interior materials are used as main index for soundproofing helicopter interiors (Li & Xuan, 2017).

1. Methodology

1.1. Importing the model

Primarily designing the Gazelle helicopter model using Autodesk Inventor. After the design phase, it is important to check all the details before importing the model. To begin, with – interface to monitoring materials physical database and mechanical properties, mathematical input parameters and finally the models. Except the model, setting all the other parameters to default. The module can also operate with geometry imported from third-party CAD software. It enables to correct geometry deficiencies to modify or simplify the geometry model. The import of a part's material properties is available in ANSYS library or in Inventor. The statistics of geometry used are 2 bodies, 723 Node, and 1755 Element.

1.2. Setting boundary conditions

Furthermore, a mathematical model is described, based on the type of analysis to be used in the work, and the required calculation module is selected (Wang et al., 2020). For example, use the Static Structural Module to calculate a structure's stress-strain state (SSS) under the impact of static loads. At this point, the characteristics of the materials, the boundary and initial conditions of the topic must be set, calculation methods selected, the solver configured in accordance with the accepted physical and mathematical model and the calculation accuracy required (Slide Player, 2019). In our case, a special Harmonic-Acoustic module was purchased. Unlike the old Ansys version, the special Harmonic-Acoustic module allowed the authors to count everything in one module. In the old Ansys, 5 modules were required and that is time consuming. So, initially the introduction of the computational domain. Computational domain is where the Authors evaluated the model, as the surface is infinite, then the computational domain was brought to give the helicopter some boundaries. And all the computation and calculation take place in the computational domain. The more complex and wide computational structure is, the longer the time that ANSYS needs to complete the simulation process. The acoustic space around the helicopter (represented as a domain) is a square. According to NASA (Noonan et al., 2001), wall disruptions were minimal, so the authors excluded them from our investigation. The helicopter was placed in a computational box. The box region represented freestream flow (Figure 1) and ensured minimal wall interference for the helicopter model and air as a material. Physical space (the actual helicopter) is presented as a solid body consisting of steel and an insulating material with some physical and mechanical properties that are averaged over (see Figure 2).

The estimation method is completely automated, but monitoring of the decision process is recommended: track

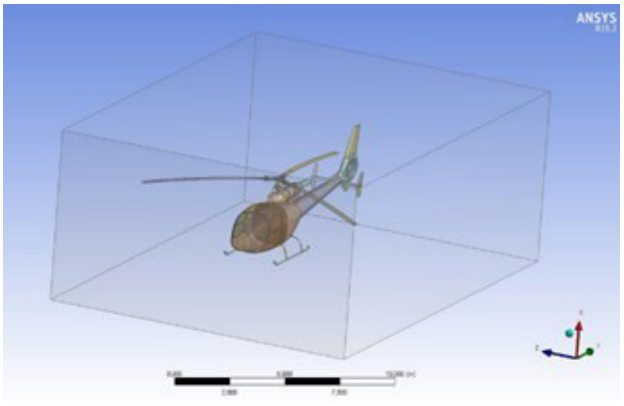

Figure 1. 3D Gazelle helicopter in domain after importing

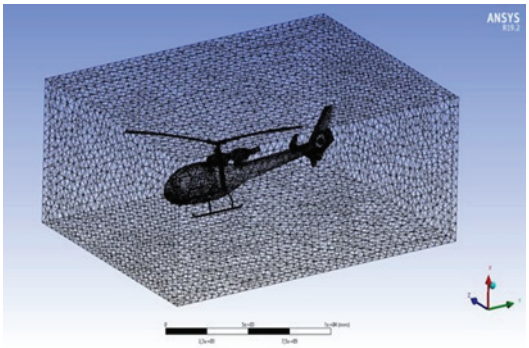

Figure 2. Result of mesh in domain Create a grid of finite elements

Figure 3. Gazelle 3D model after mesh

the solution's behavior and its compliance with the integration requirements, show external parameters on the screen that enable you to determine the solution's required quantitative characteristics, etc.

The corresponding loads and boundary conditions shall be set when solving vibroacoustic problems. First, these are types of sound energy that can be posed as a plane wave (it has the form of a plane on its front), monopole, dipole etc.

1.3. Introducing finite element meshing

Following the Authors presented data concerning the mesh, Table 1, and Figure 3.

This can be achieved using the CFD Modules for Meshing and ICEM. ANSYS started designing it when ANSYS system crashed a minor desk creating ICEM grid algorithms, and the algorithms slowly started to use in the ANSYS native system (see Figure 4).

Mesh geometric quality is defined by mesh quality, element aspect ratio, and element skewness. Figure 4a showed the mesh quality metrics imported from ANSYS, Figure 4b showed aspect ratio Quality, and Figure 4c showed Element skewness.

Table 1. Statistics of geometry used

Number label	Structural steel	Air
Nodes	16800	55500
Elements	8000	167500

1.4. Calculation inputs

To begin with the calculation, it is necessary to give the necessary inputs. The calculation method is completely automated, but monitoring of the decision process is recommended: track the solution's behavior and its compliance with the integration requirements, show external parameters on the screen that enable you to determine the solution's required quantitative characteristics, etc. The results need to be analyzed once the calculation is complete. Following is the basic input that needs to be added in-order for the calculation to take place (Abdelghani et al., 1999). The precession of the result is independent from the grid variety but depends on the grid configuration intensity. Also, like most of the common calculation, it depends on how many times it occurs. Roughly each set of calculations are repeated on the software solver by around 100 of times, hence getting a more precise answer. But by increasing the number of occurrences, there is a good chance of reducing it. Based on the work of Light hill, Proudman derived computational expressions to estimate the noise pressure of low Mach iso-tropic turbulence in terms of turbulence kinetic energy as well as dissipation period. Centered on the analogy of Proudman,

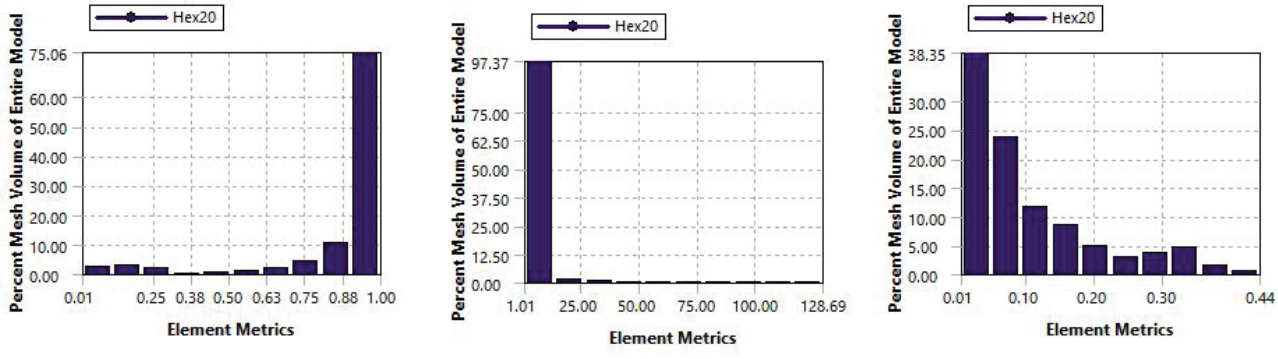

(a) (b) (c)

Figure 4. Mesh quality metrics

the flow-induced acoustic strength can be represented in compliance with normal steady-state variables which correspond to turbulent kinetic energy, k and dissipation rate, which is conventionally used in CFD. The flow noise origins may be represented as a first approximation as the number of the volume and surface components as follows:

$$P = Ps + Pv; \quad (1)$$

$$P = \int Ps\,(yb)dS + \int Pv\,(y)dV, \quad (2)$$

where: P = the total acoustic power generated by the flow; Ps (yb) = the surface component (dipole).

Pv (y) = volume component (quadrupole); (y) = the position vectors of the volumetric.

(yb) = the position vectors of the surface source point.

By considering simple spectra for the volume and surface sources, the spectral properties of the acoustic power, intensity, and therefore sound pressure can be estimated. The range for the volume sources is specified by:

$$fv(\omega,qv,rv,cv) = \frac{cv\left(\frac{\omega}{w0}\right)^{qv}}{1+\left(\frac{\omega}{w0}\right)^{\gamma v}}, \quad (3)$$

where: C_v = a parameter to be determined by model calibration.

ω = the radian frequency; ω_0 = the characteristic frequency and here is given by,

$$\omega_0 = F_v\,(\varepsilon/k), \quad (4)$$

where: F_v = a calibration pre-factor.

And the surface spectra, qs, rs and ss are parameters to be deter-mined by model calibration. The following equations are used for the acoustic power:

$$P(\omega) = Psf\,((\omega, qs, rs, ss, Cs) + Pvf\,(\omega, qv, rv, cv). \quad (5)$$

The following equations are used for the intensity spectra:

$$I\,(x, \omega) = Isf\,((\omega, qs, rs, ss, Cs) + Ivf\,(\omega, qv, rv, cv). \quad (6)$$

The correlation coefficients, *A, B, Cv, Cs, Fv, Fs, qs, rs* and *ss*, from Equations (1), (2), (3), (4) and (5) are determined through model calibration. A k–ε sound model based on the formula of Proudman was presented, which was extended to include the sound produced by a smooth body immersed in turbulent flow.

1.5. A different approach for noise prediction

After doing some research, the authors found out the SOLIDWORKS Fluid Simulator demonstrated the noise analysis capabilities. This helps the consumer to quantify the noise that the turbulent flow produces. There are now two new outcome functions available – acoustic power and sound power level. SOLIDWORKS Flow Simulation makes use of the Proudman formula for estimating noise estimation. It involves the assessment of the wideband noise generated by turbulence. In the Proudman formula the premises are as follows: High numbers flow to Reynolds, Low Mach flow, Turbulence isotropy and Zero Mean Movement. Without operator feedback the solver conducts a noise analysis measurement internally. The output parameters for the noise prediction can be allowed via the dialog window Modify Function Chart. In the following types of analysis such parameters can be used: cut plots, surface plots, iso-surfaces, fluid trajectories, point parameters, surface parameters, volume parameters, and XY plots. Using SOLIDWORKS 2020 premium version, the authors could use the full benefits of the calculations.

2. Results

2.1. Presenting the results

First to select the plane, in our case it is the right plane. And then select the required value; in the assigned case, it is the acoustic power and acoustic power level. And then select the number of legends. Then, the data will be processed, and the results will appear on the model. There can be seen the difference in different areas of the model (Gazelle). Moving on to see the flow trajectories, the following steps should be taken:

1. After initially hiding the acquired cut plot, right click on flow trajectories and click insert.
2. Then select the surfaces where it is possible to see the impact, in this case it will be the cabin area of the helicopter model.
3. After that under the appearance tab, select the representation of the flow trajectories path. Selected lines with arrow for easy understanding, and underneath can select how many lines for flow trajectories you need.
4. Then select the required parameter to use, in our case acoustics. Then click ok to see it results, after the processing the results will appear on the model.

2.2. Results from the original Gazelle model

All the methodology and procedure of how the results are obtained are shown above in the (1.2), the Gazelle helicopter is in Cruise condition flying at a speed of 264m/s, the cut plot illustration below shows the acoustic power level obtainedat a different point of the helicopter taking the right plane as frame of reference. The index depicts the maximum and minimum value of acoustic power level (dB) attained in the process (see Figure 5). The flow trajectory plot illustrated below shows the flow of turbulent air passing through the computational domain whichwas prepared initially. And the arrows represent the flow of air against the helicopters structure and attaining different acoustic power levels at different part of the helicopter. The index depicts the maximum and minimum values attained through the process (see Figure 5).

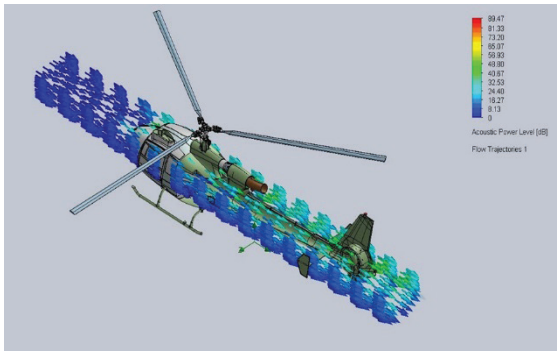

Figure 5. Flow trajectory acoustic power level default material Gazelle

Surface plot of the acoustic power level shows more detailed view of the effect on the cabin compartment of the helicopter. Taking into consideration the variation in different parts of the helicopter cabin, the acoustic power level tends to vary. The index depicts the variation in the acoustic power level (dB) (see Figure 6).

The goal plot, which is depicted below shows, the average total pressure, average total temperature, average velocity, liftforce in the Y-direction, friction force from the helicopter's direction of motion, as well as normal force. The plots are based on number of Iteration (in the Y direction) and Normalized scale of 0 to 1 (in X direction). The index of the graphis given below the graph plot (see Table 2, Figures 6 and 7).

Table 2. Ambient condition for original material Gazelle analysis

Thermodynamic parameters	Static Pressure: 101325.00 Pa Temperature: 293.20 K
Velocity parameters	Velocity vector Velocity in X direction: 264.000 m/s Velocity in Y direction: 0 m/s Velocity in Z direction: 0 m/s
Turbulence parameters	Turbulence intensity and length Intensity: 0.10 % Length: 0.030 m

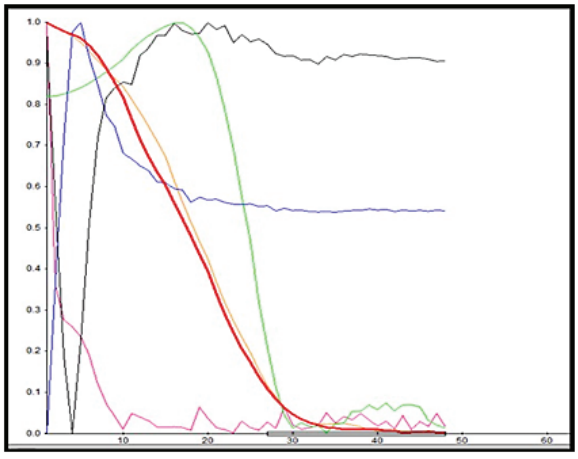

Figure 6. Goal plot default material Gazelle

The achieved IT (sound intensity) represents the number of iterations that took place to attain the results. It depicts the average value of each of the goals which were set.

2.3. Results from the aluminum Gazelle model

All the methodology and procedure of how the results are obtained are shown above in the (1.2), the Gazelle helicopter is in Cruise condition flying at a speed of 264 m/s, the cut plot show below shows the acoustic power level obtained at different point of the helicopter taking the right plane as frame of reference. The index depicts the maximum and minimumvalue of acoustic power level (dB) attained in the process (see Figure 8).

The flow trajectory plot illustrated below shows the flow of turbulent air passing through the computational domain whichwas prepared initially. And the arrows represent the flow of air against the helicopters structure and attaining different acoustic power levels at different part of the helicopter. The index depicts the maximum and minimum values attained through the process (see Figure 10).

Surface plot of the acoustic power level shows more detailed view of the effect on the cabin compartment of the helicopter.

Taking into consideration the variation in different part of the helicopter cabin, the acoustic power level tends to vary. The index depicts the variation in the acoustic power level (dB) (see Figures 9, 10 and 11).

The goal plot, which is depicted below shows, the average total pressure, average total temperature, average velocity, liftforce in the Y-direction, friction force from the helicopter's direction of motion, as well as normal force. The plots are based on number of Iteration (in the Y direction) and Normalized scale of 0 to 1 (in X direction). The index of the graphis given below the graph plot.

The graphical representation plot of the acoustic power level shown is based on the trajectory length (m) and acoustic power level (dB). It depicts the different trajectories that were passing along the helicopter showing the maximum acoustic power level achieved in the process. The trajectory is based on the opposite movement of the helicopter where the flow of air is intense (see Figure 12).

The graphical representation plot of the acoustic power shown is based on the trajectory length (m) and acoustic power level (W/m^3). It depicts the different trajectories that were passing along the helicopter showing the maximum acoustic power level achieved in the process. The trajectory is based on the opposite movement of the helicopter where the flow of air is intense.

Name	Current Value	Progress	Criterion	Averaged Value
GG Average Total Pressure 1	149572 Pa	Achieved (IT = 46)	36.5492 Pa	149576 Pa
GG Average Total Temperature 2	327.787 K	Achieved (IT = 48)	2.2011e-05 K	327.787 K
GG Average Velocity 3	263.295 m/s	Achieved (IT = 47)	0.101929 m/s	263.309 m/s
GG Force (Y) 5	-842.27 N	Achieved (IT = 40)	236.025 N	-830.515 N
GG Friction Force (X) 6	88.9687 N	Achieved (IT = 43)	1.98894 N	89.5729 N
GG Normal Force 4	5862.56 N	Achieved (IT = 40)	449.796 N	5868.51 N

Figure 7. Goal plot index (Original material Gazelle)

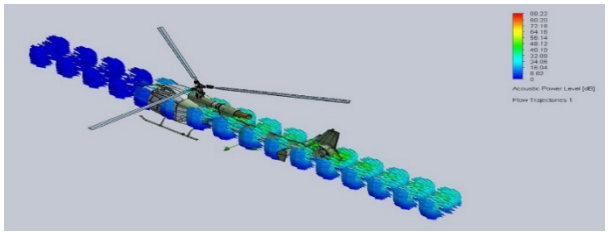

Figure 8. Flow trajectory acoustic power level aluminum material Gazelle

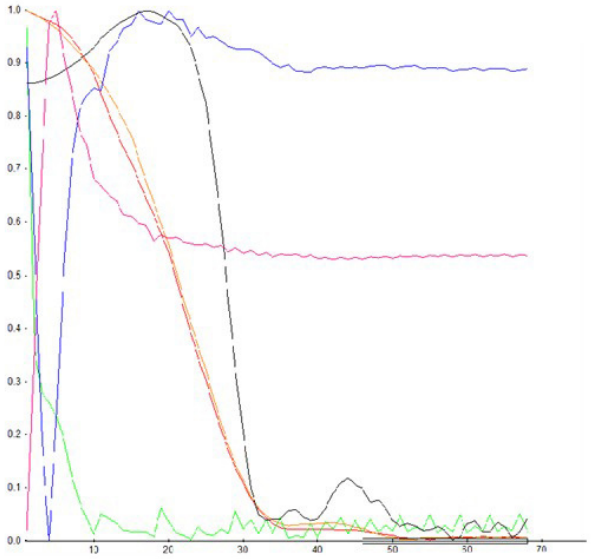

Figure 9. Goal plot aluminum material Gazelle

Name	Current Value	Progress	Criterion	Averaged Value
GG Average Total Pressure 1	149647 Pa	Achieved (IT = 52)	17.0454 Pa	149648 Pa
GG Average Total Temperature 2	327.787 K	Achieved (IT = 68)	9.00622e-06 K	327.787 K
GG Average Velocity 3	263.505 m/s	Achieved (IT = 52)	0.0450126 m/s	263.504 m/s
GG Force (Y) 5	−847.214 N	Achieved (IT = 44)	149.676 N	−845.811 N
GG Friction Force (X) 6	89.1646 N	Achieved (IT = 48)	1.26743 N	89.7475 N
GG Normal Force 4	5826.97 N	Achieved (IT = 43)	289.95 N	5823 N

Figure 10. Goal plot index – (Gazelle aluminum alloy)

2.4. Results from the Titanium Gazelle model

All the methodology and procedure of how the results are obtained are shown above in the section 2.1, the Gazelle helicopter is in Cruise condition flying at a speed of 264 m/s, the cut plot show below shows the acoustic power level obtained at different point of the helicopter taking the right plane as frame of reference.

The index depicts the maximum and minimum value of acoustic power level (dB) attained in the process (see Figure 13). Surface plot of the acoustic power level shows more detailed view of the effect on the cabin compartment of the helicopter. Taking into consideration the variation in different parts of the helicopter cabin, the acoustic power level tends to vary. The index depicts the variation in the acoustic power level (dB) (see Figure 14). The goal plot, which is depicted below shows, the average total pressure, average total temperature, average velocity, liftforce in the

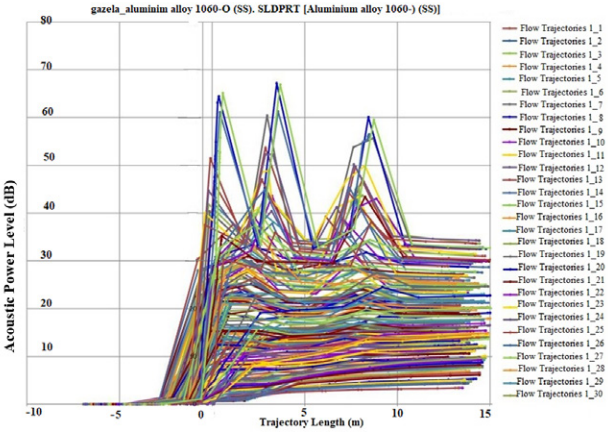

Figure 11. Acoustic power level aluminum material Gazelle

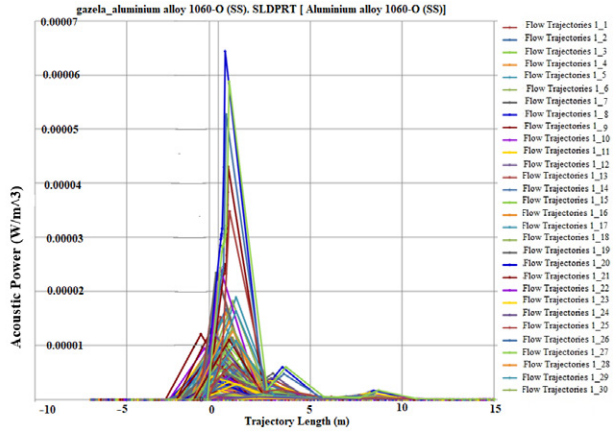

Figure 12. Acoustic power level aluminum material Gazelle

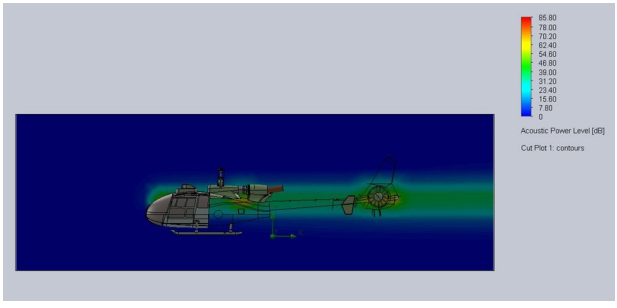

Figure 13. Cut plot acoustic power level titanium material Gazelle

Y-direction, friction force from the helicopter's direction of motion, as well as normal force.

The plots are based on number of Iteration (in the Y direction) and normalized scale of 0 to 1 (in X direction). The index of the graph is given below the graph plot (see Figure 15).

The achieved IT (sound intensity) represents the number of iterations took place to attain the results. It depicts the average value of each of the goals which were set. See Figure 16a and 16b.

The graphical representation plot of the acoustic power shown in Figures 16a and 16b is based on the

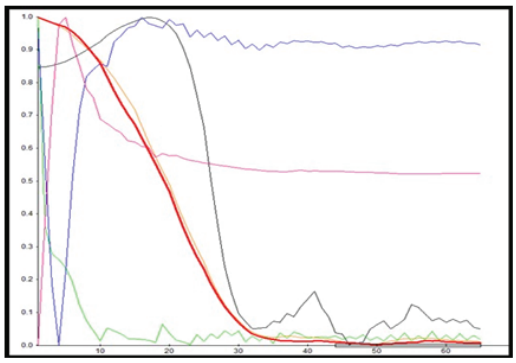

Figure 14. Goal plot titanium alloy Gazelle

Name	Current Value	Progress	Criterion	Averaged Value
GG Average Total Pressure 1	149591 Pa	Achieved (IT = 49)	26.1951 Pa	149592 Pa
GG Average Total Temperature 2	327.787 K	Achieved (IT = 65)	1.36979e-05 K	327.787 K
GG Average Velocity 3	263.377 m/s	Achieved (IT = 49)	0.0699687 m/s	263.379 m/s
GG Force (Y) 5	-797.633 N	Achieved (IT = 40)	183.289 N	-794.54 N
GG Friction Force (X) 6	89.5349 N	Achieved (IT = 43)	1.573 N	89.8664 N
GG Normal Force 4	5997 N	Achieved (IT = 40)	364.028 N	6001.31 N

Figure 15. Goal index – (Gazelle titanium alloy)

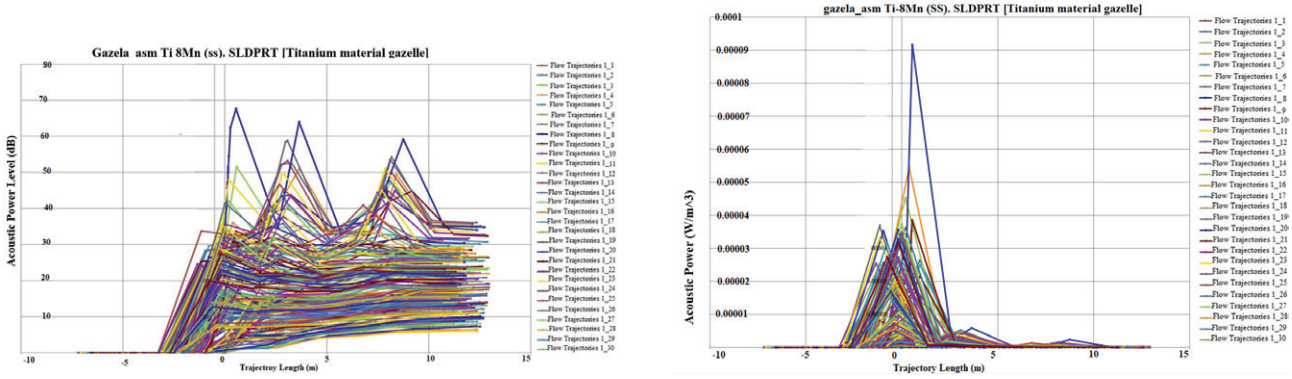

(a) (b)

Figure 16. Acoustic power level in (dB) (a) and acoustic power in (W/m^3) of titanium material Gazelle (b)

trajectory length (m) and acoustic power level (W/m^3). It depicts the different trajectories that were passing along the helicopter showing the maximum acoustic power level achieved in the process. The trajectories are based on the opposite movement of the helicopter wherethe flow of air is intense.

3. Similar approaches in Bell 429 Global-Ranger and Airbus H135 (Euro-copter EC135)

Similar approaches taken for another prototypes, Airbus H135 and Bell 429. The following are the results acquired.

3.1. Results from Airbus H135

Among the most popular passenger aircraft by Airbus Helicopters, the H135 is recognized for its large endurance, compact construction, low sound, dependability, versatility, and value-competitiveness.

This twin-engine rotorcraft can conduct several multiple objectives, landing just about anywhere, particularly high, and warm, while holding more weight than other rotorcraft in its group over greater periods.

– Results acquired from 6061 aluminum material

The plot depicted below is the results acquired after completion of 80 iterations. It depicts the sonic speed, Turbulence, length, acoustic power level, turbulent energy, cell volume, specific heat, Temperature, and dynamic viscosity. The index depicts the maximum and minimum values attained through the process. These are the cut plot results with Front plane as plane of reference (see Figure 17).

– Results acquired from the trim model Airbus H135

Airbus H135 helicopter outer material is 6016. Insulation sponge is used on the inner side. The gearbox is made of all-cast iron. The material of the gearbox was changed from 1060 to titanium as the sound level in the cabin was intense while the helicopter was flying 300 m.

The material 6016 was used as the outer material of the cabin, but the titanium was used for the inner structure, then theanalysis was performed, and it was detected that

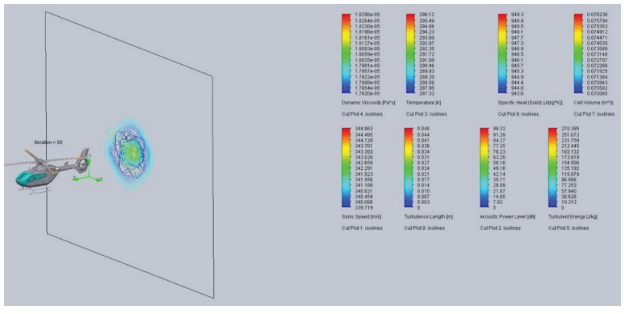

Figure 17. Values obtained for Airbus H135 first test

this way, the noise in the cabin was. However, negative consequences were detected, an increase on the outer surfaces and fatigue in the materials. To prevent this fatigue, it was decided to thinthe wall thickness and shaped the material. Due to these changes, the amount of sound (dB) in the cabin heat has decreasedand the strength of the outer material increased. Implementing insulation between the trunk and the cabin, this made surethat the sound generated in the trunk did not enter in large amount into the cabin. This also reduced the temperature valuecaused by friction in the helicopter air stream. Titanium made the aluminum used (before titanium it was 6061 aluminumalloy) surface to reduce the temperature that exposes from exterior body air friction (see Figure 18).

The graphical representation plot of the acoustic power level shown in Figure 19 and Figure 20 is based on the trajectory length (m) and acoustic power level (dB). It depicts the different trajectory that were passing along the helicopter showing the maximum acoustic power level achieved in the process. The trajectory is based on the opposite movement of the helicopter where the flow of air is intense.

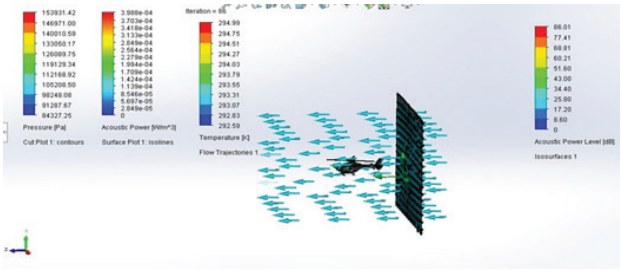

Figure 18. Values obtained for Airbus H135 second test

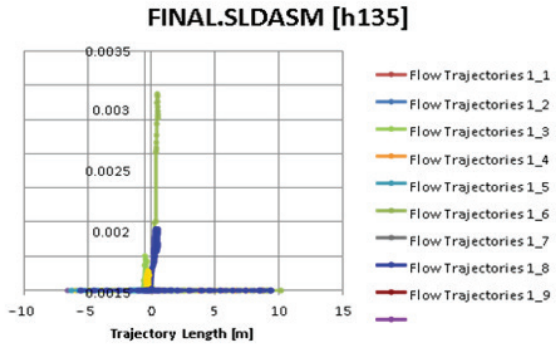

Figure 19. Acoustic power level for the final analysis Airbus H135

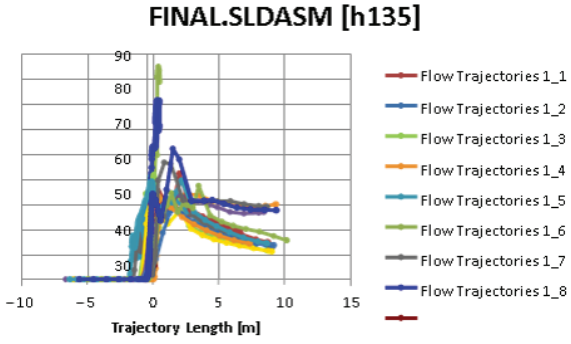

Figure 20. Acoustic power final analysis airbus H135

3.2. Results from Bell 429

– The analysis result for the default material 6061 Aluminum alloy in Bell 429 Interiors

The following plots represents the acoustic power level and acoustic power of the Bell 429. The flow trajectory passing along the helicopter represents the air flow against the helicopter motion at cruise condition. The index depicts the values, it also represents the maximum and minimum values of each (see Figure 21).

The flow trajectory depicts the turbulent air passing through the helicopter cabin. The plot defines the acoustic power, acoustic power level, turbulent energy, dynamic viscosity, pressure, temperature. The graphical representation plot of the acoustic power level shown in Figure 22 is based on the trajectory length (m) and acoustic power level (dB). It depicts the different trajectories that were passing along the helicopter showing the maximum acoustic power level achieved in the process. The trajectories are based on the opposite movement of the helicopter where the flow of air is intense (see Figure 22).

The graphical representation plot of the acoustic power shown in Figure 23 is based on the trajectory length (m) and acoustic power level (W/m^3). It depicts the different trajectories that were passing along the helicopter showing the maximum acoustic power level achieved in the process. The trajectories are based on the opposite movement of the helicopter where the flow of air is intense (Figure 23).

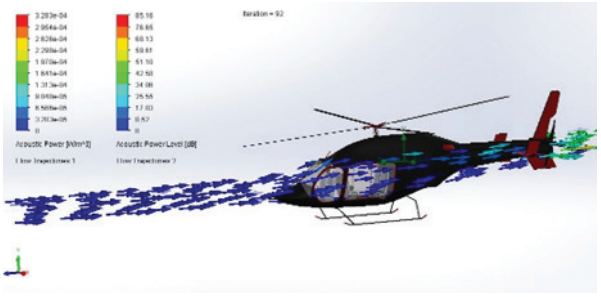

Figure 21. Bell 429 Aluminum 6061 material acoustic results

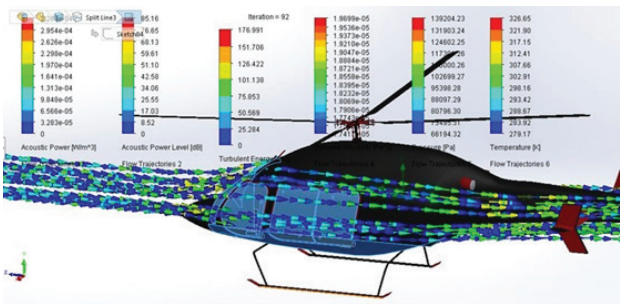

Figure 22. Bell 429 aluminum alloy 6061 overall results

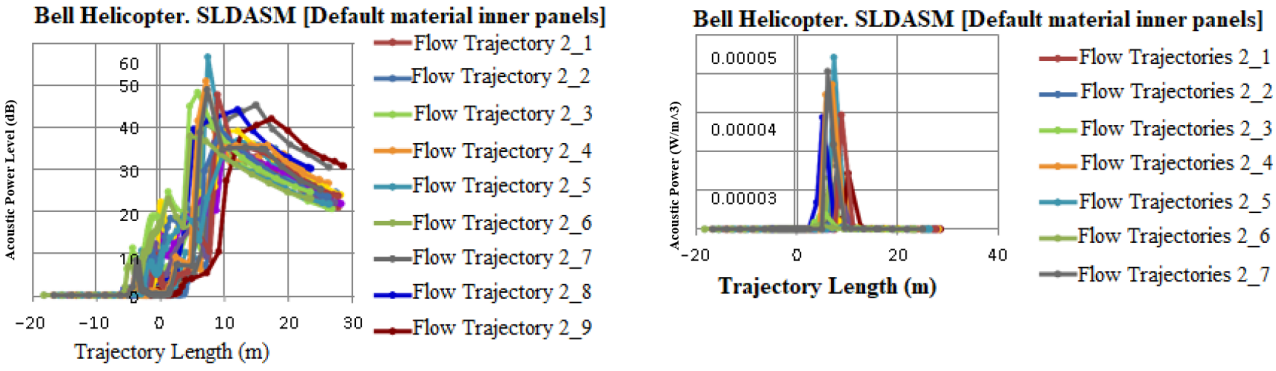

(a) (b)

Figure 23. Default Bell 429 (Al-6061), acoustic power

Conclusions

Vibroacoustic soundproofing of helicopter interiors was performed selecting a prototype. Keeping acoustic power levels and noise coefficient as measuring index helicopter interiors APL and SPL analysis has been conducted. After analysis of acoustic power level, the Authors concluded that Titanium alloy Ti-8m material as interior material for reduction of APL should be used.

The acoustic power level reduction was achieved approximately up to 7.2%. The APL simulation was performed using SOLIDWORKS 2020 software, the NDT based test on noise prediction and its impact on the acoustic power level considering the pressure and ambient temperature. Keeping Aerospatiale Gazelle as object of investigation, vibroacoustic soundproofing SPL analysis for helicopter interiors were performed using ANSYS special harmonic acoustic module. A decision was made to make changes in frequency ranges and perform the test of the frequency level from the minimum to the highest recommended frequency level which is 2000 Hz for Gazelle helicopter. The aim of the soundproofing was compared for two different sound absorption coefficient materials (SACM). 0.92 SACM and 0.7 SACM, where the two different materials were used to insulate the sound and to achieve the soundproofing. The Harmonic acoustic module focusses on the noise generated on the panels and the noise generated due to vibrations affecting interior acoustics of helicopter. The results were obtained for both the SACM materials and were taken through a series of comparisons.

Starting with the Sound Pressure level (SPL) values, acoustic total velocity, frequency band SPL, and all these results were again carried out through an A-weighted testing to get a more precise finding and accuracy. From the results acquired for both SACMs; it was clear that higher valued 0.92 SACM showed a better uniform soundproofing through varied frequency range than 0.7 SACM and less distribution of acoustics once the sound enters the cabin.

Although 0.7 SACM have a very less uniformity through the frequency ranges. Considering typical cabin sound excitation to the interiors, the 0.92 SCAM was providing a uniform sound pressure level detection of approximately 10.34% and the 0.7 SACM was providing a non- uniform percentage of approximately 12.56% in different frequency ranges, these values are confirmed and verified with the A-Weighted values for more precision. The practical implementation of 0.92 SACM can be considered due to its cost effective, long lasting, and cheaper manufacturing features. Results of research reveal that the problem of interior noise in helicopters can be reduced successfully up to 10.34%. Since tests and simulations were conducted only for forward motion of helicopter in cruise condition, future work will focus on all phases of flight and in varied motions of airflow trajectory.

References

Abdelghani, M., Hermans, L., & Van der Auweraer, H. (1999). A state space approach to output-only vibro-acoustical modal analysis. In *Proceedings of the SPIE – The International Society for Optical Engineering* (Vol. 3727, pp. 1789–1793). ResearchGate.

Agusta Westland European Aviation. (2013). *Safety agency operational evaluation board report*. Köln, Germany.

Airvectors. (2021). *Sud aviation gazelle helicopter.* http://www.airvectors.net/avgazel.htmlfonds

Buning, P., G., & Pulliam, T., H. (2011, June 27–30). Cartesian off-body grid adaption for viscous time accurate flow simulation. In *20th AIAA Computational Fluid Dynamics Conference (AIAA 2011-3693)*. Honolulu, Hawaii. Aerospace Research Central. https://doi.org/10.2514/6.2011-3693

Globalair. (2020). *Aerospatiale Gazelle SA 341*. https://www.globalair.com/aircraft-for-sale/Specifications?specid=1592

Helicopter University. (2018). *Helicopter rotor limitation during forward motion.* https://helicopteruniversity.files.wordpress.com/2018/02/text_2004_10_28_hubschrauber-1-161.jpg?w=748

Holst, T., L., & Pulliam, T. H. (2009, June 22–25). Overset solution adaptive grid approach applied to hovering rotorcraft flows. In *27th AIAA Applied Aerodynamics Conference*. San Antonio, TX. https://doi.org/10.2514/6.2009-3519

Li, Y., & Xuan, Y. (2017) Thermal characteristics of helicopters based on integrated fuselage structure/engine model. *International Journal of Heat and Mass Transfer, 115*, Part A, 102–114. https://doi.org/10.1016/j.ijheatmasstransfer.2017.07.038

Lu, Y., Wang, F., & Ma, X. (2018). Helicopter interior noise reduction using compound periodic struts. *Journal of Sound and Vibration, 435*, 264–280. https://doi.org/10.1016/j.jsv.2018.07.024

Lu, Y., Wang, F., & Ma, X. (2017). Research on the vibration characteristics of a compound periodic strut used for a helicopter cabin noise reduction. *Shock and Vibration, 2017*. https://doi.org/10.1155/2017/4895026

Meakin, R. L. (1995, June 19–22). An efficient means of adaptive refinement within systems of overset grids. In *The 12th Computational Fluid Dynamics Conference (Paper AIAA-1995-1722)*. San Diego, CA. https://doi.org/10.2514/6.1995-1722

Mucchi, E., Pierro, E., & Vecchio, A. (2012). Advanced vibro-acoustic techniques for noise control in helicopters. In D. Siano, *Noise control, reduction and cancellation solutions in engineering*. IntechOpen. https://doi.org/10.5772/27797

Noonan, K. W., Yeager Jr, W. T., Singelton, J. D., Wilbur, M. L., & Mirick, P. H. (2001). *Wind tunnel evaluation of a model helicopter main-rotor blade with slotted airfoils at the tip (NASA TP-2001-211260)*. NASA.

Pierro, E., Mucchi, E., Soria, L., & Vecchio, A. (2009). On the vibro-acoustical operational modal analysis of a helicopter cabin. *Mechanical Systems and Signal Processing, 23*(4), 1205–1217. https://doi.org/10.1016/j.ymssp.2008.10.009

Park, M. A. (2011, June 27–30). Low boom configuration analysis with FUN3D adjoint simulation framework. In *The 29th AIAA Applied Aerodynamics Conference (AIAA-2011-3337)*. Honolulu, HI. https://doi.org/10.2514/6.2011-3337

Slide Player. (2019). *Aerodynamic performance helicopter* [slides]. https://slideplayer.com/slide/3493118/

Simon, D., R., & Savage, J. C. (1975). *Flight test of the Aerospatiale SA-342 helicopter.* Army Air Mobility Research and Development laboratory Fort Eustis Va Eustis Directorate. https://doi.org/10.21236/ADA016921

This Day in Aviation. (2021). *Fenestron Gazelle helicopter*. https://www.thisdayinaviation.com/tag/fenestron/

Vario Helicopter. (2020). *Gazelle Westland Variable*. https://www.vario-helicopter.biz/de/images

Wang, F., Lu, Y., Lee, H. P., Yue, H. (2020). A novel periodic mono-material strut with geometrical discontinuity for helicopter cabin noise reduction. *Aerospace Science and Technology*, *105*, 105985. https://doi.org/10.1016/j.ast.2020.105985

Wikipedia. (n.d.). *Helicopters*. https://en.wikipedia.org/wiki/Main_Page

Yamauchi, G. K. (2018). *A Summary of NASA Rotary Wing Research*: *Circa 2008–2018*. Ames Research Center Moffett Field, California.